CEAS Aeronautical Journal
https://doi.org/10.1007/s13272-024-00783-1

ORIGINAL PAPER

Testing of an indirect ice detection methodology in the Horizon 2020 project SENS4ICE

C. Deiler[1]

Received: 13 December 2023 / Revised: 15 October 2024 / Accepted: 15 October 2024

Abstract
Supercooled large droplets (SLD) icing conditions have been the cause of severe aircraft accidents over the last decades. Existing countermeasures, even on modern airplanes, are not necessarily effective against the resulting ice formations, which raises a demand for reliable detection of SLD in all conditions for safe operations. The EU-funded Horizon 2020 project SENS4ICE focused on new ice detection approaches and innovative sensor hybridization to target a fast and reliable (SLD-)ice detection. The performance-based (indirect) ice detection methodology is key to this approach and based on the changes of airplane flight characteristics under icing influence. This paper provides a short overview of the development and implementation of the indirect ice detection (IID) algorithms in SENS4ICE. Moreover, it gives and discusses first exemplary results from the IID tests in classical icing conditions during the SENS4ICE North America flight test campaign conducted in February/March 2023 out of St. Louis Regional Airport in Alton (Illinois, USA).

Keywords Aircraft icing · Aircraft flight performance · Ice detection · Flight test data evaluation

Nomenclature

b_T	Engine model adjustment offset value N
C_D	Drag coefficient
C_{D0}	Zero-lift drag coefficient
$\Delta C_{\widetilde{D}}$	Equivalent drag coefficient
ΔISA	Temperature offset to standard atmosphere K
E	Energy J
$\dot{E}_{\text{tot}}$	Energy change/power imbalance W
$\dot{E}_{\text{tot,ref}}$	Reference power imbalance W
f_T	Engine model adjustment factor
H	Altitude, m
k_1, k_2	Drag coefficient equation factors
LWC	Liquid Water Content g/m^3
m_{AC}	Aircraft mass, kg
MVD	Median Volumetric Diameter microns
$\mathcal{P}$	Percentile/quantile
$\overline{q}$	Dynamic pressure, Pa
S_{Wing}	Wing surface area, m^2
T	Engine thrust force, N
V_{TAS}	True airspeed, m/s
α	Angle of attack, rad
HIDS	Hybrid Ice Detection System
IID	Indirect Ice Detection
IPS	Ice Protection System
SLD	Supercooled Large Droplets

✉ C. Deiler
christoph.deiler@dlr.de

[1] DLR (German Aerospace Center), Institute of Flight Systems, Lilienthalplatz 7, 38108 Braunschweig, Germany

1 Introduction

Icing can have hazardous effects on airplane performance characteristics and can be a limiting factor for the safe flight envelope. The change of the dynamic behavior and potential premature stall raise the need for pilot situational awareness and an adaption of control strategy. Different accidents worldwide have shown the criticality of icing-related aircraft characteristics degradations, e.g., Refs. [1–4], especially when caused by supercooled large water droplets (SLD). Although in most cases, the involved aircraft were equipped with state-of-the-art ice protection systems, the hazardous effects of SLD ice accretion often led to catastrophic events, i.e., due to ice accretion outside the protected areas. These icing conditions can pose a high risk to the aircraft, crew, and passengers, which requires specific detection and countermeasures to assure aircraft safety during flight. The certification of (modern) transport aircraft for flight into (known) icing conditions was mainly based on the certification requirements given in the so-called App. C to,

Published online: 19 November 2024

e.g., CS-25 [5]. Though, with the identified hazard to fixed-wing aircraft resulting from SLD, the certification requirements were extended by the new App. O including SLD ice [6]. From now on, manufacturers must prove that a newly developed airplane is also safe for flight into the even more hazardous SLD icing conditions. For flight safety, it is now mandatory to detect the presence of SLD icing very early after the encounter. Furthermore, monitoring the aircraft's remaining capabilities during the further flight (in icing conditions) would give a relevant information to the pilots about the required adaption of operation, e.g., urgent need to enter warm air to melt the ice accretion on the airframe in case the aerodynamics are significantly degraded. As a complicating fact, predicting the distinct change of aircraft characteristics caused by SLD ice formation is challenging and still topic of current aviation research.

Most of the existing ice protection systems (IPS) on transport aircraft require a significant amount of energy provided on board. Thermal ice protection systems usually rely on bleed air, which reduces the engine effectiveness and increases fuel consumption of the engines. Using such a system preventively has a direct impact on fuel consumption and therefore aircraft emissions as well as operation cost. A more deliberate activation of the IPS can lead to more efficient but safe flight operations for which a reliable information about, e.g., the IPS effectiveness against the current icing encounter would be necessary. This information could be provided by suitable ice detection methods giving a hint about the presence of icing conditions, actual ice formation on the airframe, and the effect on the flight characteristics [7, 8]. Moreover, it would also open possibilities for the modification of existing systems by modulating the thermal power according to the current need, directly reducing the energy consumption and increasing the aircraft efficiency.

The goal of the European Union Horizon 2020 Project "SENSors and certifiable hybrid architectures for safer aviation in ICing Environment" (SENS4ICE) is to provide a more comprehensive overview of the icing conditions, ice formation, and aircraft degradation status including the aircraft's remaining capabilities (icing-related change in aircraft flight physics, i.e., degraded aircraft performance) [9, 10]. In a layered approach, a hybrid ice detection system (HIDS) is forming the core function accompanied by additional new nowcasting and enhanced weather forecasting [11, 12]. The latter allows initially preventing the flight through hazardous icing conditions from a strategic and tactical point of view, whereas the hybrid detection architecture provides the necessary information to the flight crew for IPS activation and execution of safe exit strategies, when required. It combines in-situ measurement from various ice detection sensor technologies based on different physical principles (optical or remote sensing and ice accretion detection, e.g., see Refs. [13, 14]) with an indirect detection methodology. Hence, the HIDS allows giving a more general overview of the current aircraft icing than an individual system alone. In addition, the indirect detection methodology monitoring the current aircraft flight characteristic reveals the degraded aircraft flight envelope, which is essential for loss of control prevention. An overview of the layered safety concept is given in Fig. 1. The concept targets a general application and safety enhancement for fixed-wing aircraft icing and is not only dedicated to aircraft already certified for flight into known icing conditions (App. C). It intentionally goes beyond current certified aircraft systems proving safe operations in icing conditions [15].

Within SENS4ICE, the "indirect ice detection" (IID) was further developed and matured and is one important project pillar [8]. It is a novel methodology and system for the onboard surveillance of aircraft flight performance used for ice detection purposes. It was originally formulated and presented as a performance-based ice detection methodology, e.g., in Ref. [7]. It utilizes the effect of aircraft performance degradation due to ice accretion. The idea of the IID is not restricted to an application on large transport aircraft but can also enable a reliable ice detection for aircraft systems, such as small UAV, which currently have no ice detection system, but operate in hazardous environments with very different icing conditions.

The SENS4ICE project contained two major icing flight test campaigns: the North America campaign using an Embraer Phenom 300 prototype aircraft and the European campaign with an ATR 42-320 operated by SAFIRE [10, 16, 17]. Herein, the first evaluation results from the North America fight test campaign are presented, which were conducted between February 22nd and March 10th 2023 out of St. Louis Regional Airport (Alton, IL, USA) with a focus on the IID ability to reliably detect the performance degradation caused by icing during several example ice encounters. As SLD icing conditions have a low probability compared to other App. C conditions, it was very difficult to obtain any SLD encounters during the flight test campaign. For the presentation of flight test results and the IID response to airframe icing during the campaign, examples from two of the first flights with suitable icing encounters in App. C

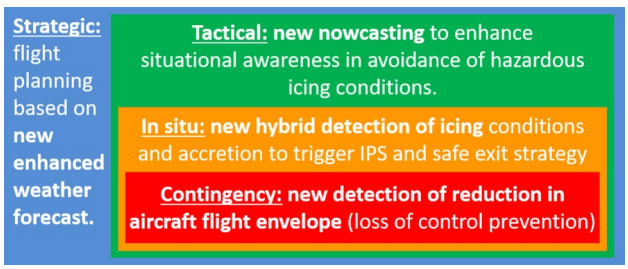

Fig. 1 SENS4ICE layered safety concept

(two encounters) and App. O (one encounter) were selected. It is important to mention that with the SENS4ICE project and the results presented herein, the performance-based ice detection methodology inside the IID was demonstrated the first time in flight through natural icing conditions.

The paper is structured as follows:

- A brief description of the indirect ice detection methodology based on the observed aircraft flight performance variation is given in Sect. 2;
- Section 3 contains the specific implementation of the detection algorithm for the SENS4ICE purpose with focus on the Embraer Phenom 300 test aircraft;
- Exemplary flight test data analysis from first demonstration of the IID in flight during the SENS4ICE North America icing flight test campaign reflecting the system performance with regard to the ability of reliable ice detection in Sect. 4.

Finally, a summary with initial conclusions as well as an outlook are given.

2 Airframe ice detection through flight performance monitoring

One major effect of aircraft ice accretion is a significant drag increase due to surface roughness changes, parasitic influence of ice protuberances, and local flow separation. Another effect of icing is a change of the aircraft lift behavior, causing, e.g., earlier or more abrupt flow detachment with increasing angle of attack and/or a reduction in aircraft lift slope. Both together significantly alter the aircraft flight performance which can be monitored during flight. Figure 2 illustrates the typical icing-induced change of the lift and drag curves as generally described, e.g., in the AGARD report 344 [18]. Icing will also change the aircraft's flight dynamics (e.g., pitching and rolling moment). In addition, the control characteristics are negatively affected by icing

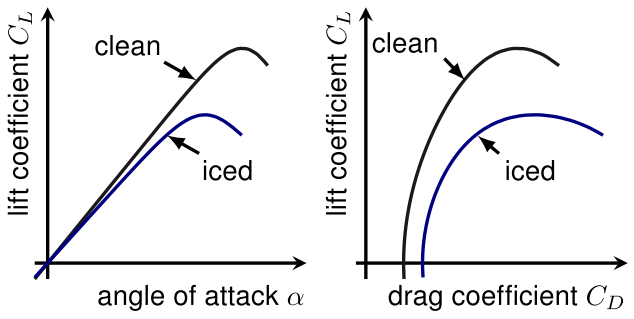

Fig. 2 Expected icing influence on aircraft aerodynamics (lift and drag coefficient); adapted from [18]

and change the aircraft dynamics differently according to the specific occurrence of ice accretion. However, these changes are very difficult to detect during flight. The IID relies on the icing-related change of aircraft flight performance [7, 8].

Hence, aircraft flight performance monitoring can provide crucial information to the pilots about the current (limited/degraded) aircraft capabilities, e.g., reduced maximum climb performance or reduced specific excess power, while only requiring the sensor information that is available on all modern airliners and business jets. As an advantage, the developed methodology relies only on the change in flight performance (i.e., steady flight states), which is contrary to the many other attempts (e.g., in Refs. [19–24]) based on the estimation of changes in the aircraft's dynamic behavior or a combination of both. However, the change in dynamic aircraft behavior caused by icing is not uniform to reliably conclude on icing as shown in, e.g., Refs [25, 26]. In addition, with focusing on the effects of icing on flight dynamics, the essential part of altered flight performance is not covered [7]. The change/degradation of flight performance is an indicator of ice accretion that is both robust and highly available: unlike the approaches based on the detection of changes in the aircraft dynamical behavior, it can be used also during steady flight conditions (most of an operating flight) and can detect icing effects significantly before entering into stall. Although other direct ice measuring approaches for the detection of icing conditions or ice accretion on the airframe could deliver a partly similar information, the indirect detection using the performance monitoring approach would not require (potentially costly) modifications of existing and future aircraft. It is important to highlight that the method within the IID is focused on the flight performance changes without any specific need for additional dynamic aircraft excitations. Classical dynamic excitations with larger amplitudes, like for system identification purposes, are not acceptable during normal operations as stated in Ref. [21]. However, there is also work done indicating that the impact of these excitations can be kept to a minimum [27]. In addition, in case of icing, it must be kept in mind that dynamic excitations can be critical when flying with an aircraft that has a reduced (unknown) maximum-lift angle of attack.

The basic assumption for the indirect ice detection using performance monitoring is the possibility to discriminate between (very slow and low) performance variation of a single aircraft over lifetime in service (or within a fleet of same type) and the (much faster) performance variation caused by icing. Factors causing the flight performance variations across airplanes from the same type are for example

- production tolerances,
- aircraft skin repairs,
- aircraft skin contamination (e.g., dirt),
- engine aging causing reduced efficiency, or

- engine contamination.

The aircraft flight performance can be seen as follows:

Flight Performance = Nominal Aircraft Performance
+ Expectable Variation
+ Variation to be detected

whereby the "Expectable Variation" part gathers the effects mentioned previously and the "*Variation to be detected*" is subject to the indirect ice detection approach. The first step is to determine the typical and most extreme flight performance variation ("Expectable Variation") encountered during regular airline operations (due to a real performance variation or sensor errors). There are different approaches to reveal this variation from operational flight data. In Refs. [7, 28], the determination of the performance variation from 75,689 flights with Boeing B737 aircraft operated by a German airline is presented. The results underpinned the above-mentioned assumption and revealed that it is possible to successfully monitor the aircraft performance using the regular sensors and with a level of precision that permits detecting the performance degradation induced by the ice accretion at a very early stage (before this degradation of the performance reaches a critical level).

The flight data for the Phenom 300 prototype (Fig. 3) serving as flight test aircraft in SENS4ICE North America flight test campaign were processed to obtain the measured performance variation during flight. The resulting performance variation (without icing) of the prototype test aircraft without specific SENS4ICE modifications is given in Fig. 4, serving as a baseline performance variation evaluation. The plot contains different convex hulls including a specific quantile of the flight data used to calculate the nominal aircraft aerodynamics or flight performance respectively (including the nominal thrust model). Note that the convex hulls include aerodynamic data (lift and drag coefficient)

Fig. 3 Embraer Phenom 300 flight test aircraft: prototype aircraft with all modifications for the SENS4ICE North America flight test campaign (credit Embraer)

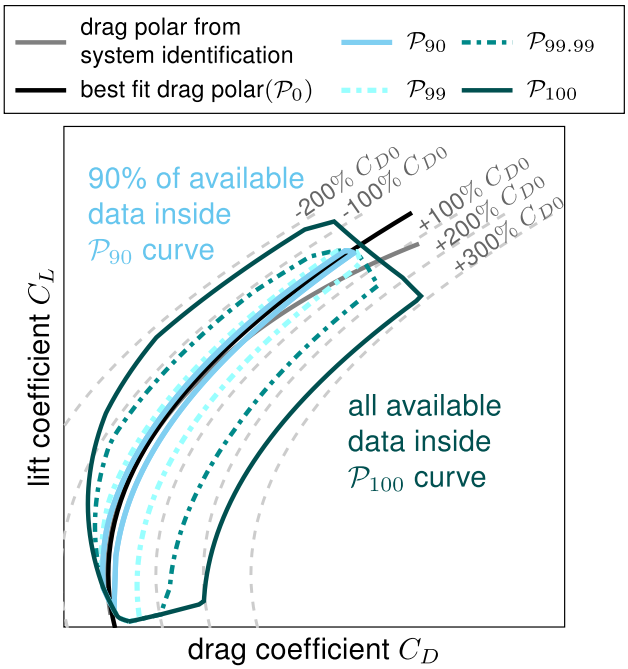

Fig. 4 Measured aircraft performance variation based on specific flight test data gathered with the Embraer Phenom 300 prototype at several flight conditions (2.2 million data points): estimated drag polar and convex hulls ($\mathcal{P}_{90}$, $\mathcal{P}_{99}$, $\mathcal{P}_{99.9}$ & $\mathcal{P}_{100}$) showing the data distribution from flight test

directly calculated from recorded flight data and are chosen for visualization, because the data variation cannot be shown by giving the individual 2.2 million aerodynamics data points: for example, the $\mathcal{P}_{90}$ curve includes 90% of the data and the $\mathcal{P}_{100}$ curve shows the extension of the area including all available data. In addition, the plot contains the best fit drag polar based on the whole data set and the drag polar resulting from a previous system identification [29, 30]. To assess the (performance) variation obtained from the flight data sets, additional indication of drag polar shifts with multiples of the zero-lift drag coefficients are given, indicating that the observable variation within the data can reach up to four times the true values or values less than zero. The measured variation in this case results from the non-filtered measurements which are also not corrected for external disturbances. Therefore, the measured variation does include (external) effects on the aircraft, e.g., resulting from encountered atmospheric disturbances or conducted maneuvers, together with additional influences on the performance calculation like measurement noise. This is in contrast to the results given in Refs. [7, 28], where the data were corrected for most of these effects. However, for the design of the IID, it is essential to also evaluate the measured performance variation of a single aircraft, which is mainly the variation between the actual aircraft and the reference model together with the named additional influences. Hence, in this

case, the 90% quantile ($\mathcal{P}_{90}$) is the most relevant, because the drag or performance variation of majority of data defines the possible detection accuracy. Furthermore, it can be reliably assumed that the remaining variation, especially the last percent of data between the 99% quantile and full data set, results from the external influence which can be ignored for the ice detection or filtered within the designed algorithm. Further information on the reference performance data and the assumptions made are given in Refs. [8, 31].

The IID is based on a quasi-steady aircraft flight performance monitoring which requires a good measurement of the current flight condition and engine parameters. If the measurements of the flight condition are available with sample rate (and frame rate for transmission to the IID) above, e.g., 20 Hz and are not filtered or corrected for, e.g., measurement noise, the IID must account for a higher observed performance variation ("Expectable Variation"). However, it is assumed to be able to reliably detect a performance degradation due to icing fast. If the rate is significantly lower (e.g., 5 Hz) and/or the data are already low-pass filtered, the IID will observe a smaller performance variation and the detection of the degradation might be slower than for the higher measurement rate case. Consequently, within the application of the IID approach, the potential detection speed and accuracy is directly related to the quality of the flight data measurements. Nevertheless, this is independent to unsteady flight conditions or dynamic flight, where the measurements can significantly vary. In this case, the IID is capable of detecting the performance variation with the same accuracy and response time as during steady flight.

The basic idea of the performance-based ice detection method is comparing the current (possibly ice-influenced) aircraft flight performance characteristics with a known reference (see Fig. 5). The flight performance can be defined as a power imbalance (change of total energy) $\dot{E}_{tot}$ for the current state and the reference, which allows representing the change of aircraft characteristics in a sole value. Consequently, this reduces the complexity of the detection algorithm. It further combines the individual parts of the aircraft performance related to aerodynamics and engines in a single observation. The power imbalance $\dot{E}_{tot}$ can be formulated as

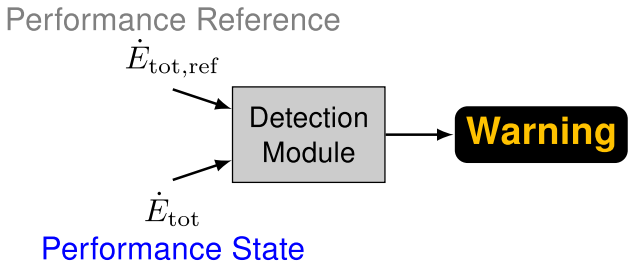

Fig. 5 Basic principle of the IID method based on the aircraft power imbalance; from [7]

$$\dot{E}_{\mathrm{tot}} = V_{\mathrm{TAS}} \cdot \dot{V}_{\mathrm{TAS}} \cdot m_{\mathrm{AC}} + \frac{1}{2} \cdot V_{\mathrm{TAS}}^2 \cdot \dot{m}_{\mathrm{AC}} + g \cdot \dot{H} \cdot m_{\mathrm{AC}} + g \cdot H \cdot \dot{m}_{\mathrm{AC}} , \tag{1}$$

with the altitude change (with respect to time) $\dot{H}$ referenced to the surrounding air, the speed change (with respect to time) $\dot{V}_{\mathrm{TAS}}$, and the change of aircraft mass $\dot{m}_{\mathrm{AC}}$ corresponding to the aircraft fuel consumption. Note that the gravitational acceleration is assumed to be constant and its variation with time can be neglected for the calculation of the power imbalance. To convert the power imbalance into an equivalent drag coefficient variation, which is easier to assess from an engineering point of view, the formulation from Ref. [7] is used

$$\Delta C_{\widetilde{D}} \mathrel{\widehat{=}} \frac{\dot{E}_{\mathrm{tot,ref}} - \dot{E}_{\mathrm{tot}}}{V_{\mathrm{TAS}} \cdot \overline{q} \cdot S_{\mathrm{Wing}}} . \tag{2}$$

This non-dimensional equivalent drag coefficient is calculated by comparison of the current determined power imbalance $\dot{E}_{\mathrm{tot}}$ and a predefined reference value $\dot{E}_{\mathrm{tot,ref}}$. The performance reference value is a function of the aircraft flight state defined by parameters like altitude, speed and load factor, the aircraft configuration (e.g., mass, high-lift system configuration), as well as the propulsion system state. If required, some corrections for additional influences, e.g., flight with side-slip condition, could be applied [7]. Furthermore, the airspeed V_{TAS} is derived from several measurements and contains a combination of aircraft flight path velocity and wind speed (both to be understood as 3D vectors). For the time derivative $\dot{V}_{\mathrm{TAS}}$, the component related to the change of wind vector should be ignored to prevent it from falsifying the performance estimate. A variable wind-corrected energy change $\dot{E}_{\mathrm{tot,corr}}$ could then be used changing $\dot{V}_{\mathrm{TAS}}$ in Eq. 1 to $\dot{V}_{\mathrm{TAS},\dot{\vec{V}}_{\mathrm{k}}}$ considering only the airspeed change related to the flight path; see Ref. [7] for a more detailed explanation.

The equivalent drag coefficient is well comparable to a predefined threshold value and indicates an abnormal performance variation when exceeding. This is further independent from any flight point. Note that a drag coefficient value is well interpretable in terms of aerodynamics and flight mechanics by aerospace engineers and allows a direct assessment of the magnitude of aerodynamic degradation caused by icing. Within the IID, this drag coefficient is normalized with the aircraft's zero-lift drag coefficient and compared to a predefined threshold. For the SENS4ICE North America flight test campaign with the Phenom 300 prototype, a threshold of 10 % is defined to provide a good sensitivity and reliability.

A simple way for the definition of the aircraft flight performance reference is the usage of a multi-dimensional table including the different above-mentioned states and

conditions as dimension [7, 8]. Another way is to calculate the reference power imbalance from an aerodynamic database and engine thrust model, if both are available. In such case, it must be determined if the variation in the reference power imbalance results from changes of the aircraft aerodynamics or the engine performance. For the implementation in SENS4ICE, an engine thrust model was available and the reference power imbalance can be formulated as a function of flight condition, aircraft configuration (using a reference aerodynamic model representation), and the current predicted engine thrust. In detail, the dot product of the thrust vector and true airspeed vector allows calculating the contribution of the thrust on the reference power imbalance. Together with the reference drag, Eq. 2 can be reformulated to include the separated models. A methodology to adapt flight performance models from operational flight data is given in Refs. [32–34], which could be relevant for the adaptation of the performance reference with separated models (aerodynamics and engine thrust). Note that the choice for the representation of the performance reference is also dependent on the requirement for adaptation to a specific aircraft, which might be easier in the table approach [7]. Further detailed information on performance-based ice detection, which is already under patent protection in several countries [35], can be found in Ref. [7].

3 Implementation of the indirect ice detection algorithm

The indirect ice detection is implemented as a modular set of functions, including the core detection algorithm, the required data preprocessing, and a subsequent detection result filtering to prevent false detections. The latter also guarantees the necessary system robustness and consequently reliability. Within SENS4ICE, the indirect ice detection is part of the HIDS developed by SAFRAN Aerosystems and allows with its specific implementation detecting performance degradations and therefore the ice accretion (see Fig. 6). The HIDS implementation is designed to be applicable to both flight test aircraft used for SENS4ICE flight test campaigns, which are very different aircraft configurations: a light business jet aircraft (Embraer Phenom 300) and a regional class turboprop aircraft (ATR 42). This applicability is possible through the generic formulation of the detection methodology itself, not relying on specific information about the aircraft: the formulation allows shifting the aircraft dependencies to another level of the implementation. This required aircraft-specific adaption of the detection is achieved by considering the aircraft-specific reference, which is an input to the algorithm and not part of the core implementation. For a more detailed description of the HIDS and its implementation, the reader is referred to Refs. [8, 36].

There are several needs for adjustments inside the IID for a specific aircraft type, mainly as part of the "Aircraft Flight Data" and "Performance Reference Database" blocks in Fig. 6:

- flight data preprocessing,
- flight performance reference database,
- indirect ice detection threshold and confirmation times and
- detection reliability conditions.

A detailed description about these required adjustments is given in Ref. [8] and the flight performance reference as well as the detection threshold and confirmation times are briefly described below.

For the SENS4ICE flight tests, the IID is implemented in MATLAB®/Simulink. The HIDS runs on a dSpace MicroAutoBox in real time for the flight tests, and the IID Simulink model can be easily transferred to this specific hardware. Anyway, for a further IID and HIDS maturation, a direct implementation in the aircraft avionics is foreseen.

3.1 Flight performance reference database

The IID relies on an accurate flight performance reference which allows computing an expected current flight performance to be compared to the measured one within the detection module. For the presented case, the IID consists of a performance reference database splitting engine and aerodynamic influence into individual parts. Having this separation,

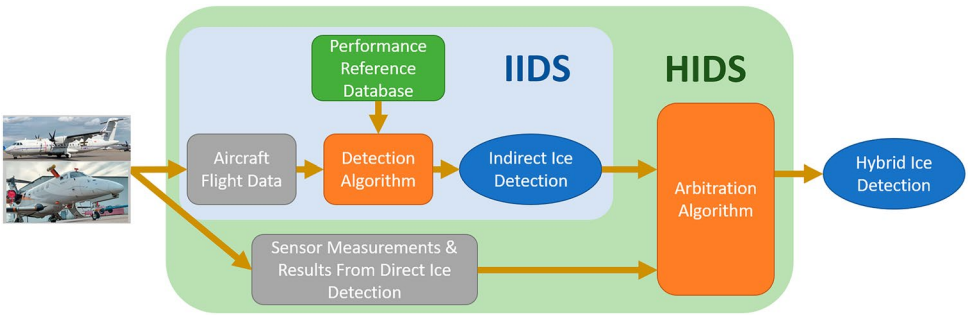

Fig. 6 Visualization of HIDS concept used within SENS4ICE (pictures credit DLR/Embraer/SAFIRE)

it was more easy to adapt the reference aerodynamics to the specific conditions given by the flight test aircraft having several external probes attached to the test aircraft influencing the aircraft's flight performance.

The flight test case-specific adaption of the aerodynamic performance reference is formulated as an additional part to the "base" aircraft reference, which allowed a very fast adaption of the reference database prior to the icing flight tests. For the North America flight test campaign, the final configuration of the aircraft with all modifications, i.e., external sensors and pods mounted on wing pylons or at the fuselage, was available for a check flight before the campaign in February 2023. Moreover, the ferry flights from Brazil, where the prototype was modified at Embraer facilities, to the United States, where the flight test campaign took place, served as an additional source of information for the corresponding changes of the aerodynamics due to aircraft modifications with SENS4ICE equipment (compared to the "base" aircraft). Using a kind of delta approach to the aerodynamic reference, it could be shown that the performance reference was successfully adapted to the modified aircraft. Having a representation of the aircraft drag polar given by

$$C_D = C_{D0} + k_1 \cdot C_L + k_2 \cdot C_L^2 \,, \tag{3}$$

a linear parameter extension was already foreseen in the IID implementation allowing the adaptation of the aircraft aerodynamics to the SENS4ICE aircraft modifications

$$\begin{aligned} C_D =& \left(C_{D0,\mathrm{ref}} + \Delta C_{D0}\right) + \left(k_{1,\mathrm{ref}} + \Delta k_1\right) \cdot C_L \\ &+ \left(k_{2,\mathrm{ref}} + \Delta k_2\right) \cdot C_L^2 \,. \end{aligned} \tag{4}$$

Figure 7 shows the drag polar calculated from flight test data of the clean air flights with the aircraft in campaign configuration together with the pre-campaign reference used to design the IID and the modified drag polar used for the icing flight tests.

Note that the flight performance reference in SENS4ICE is based on certain a priori knowledge and information obtained from a specific flight data evaluation. However, for new aircraft designs, it could also be based on the design models and initial prototype flight test results.

3.2 Detection threshold, confirmation time, and reliability conditions

A detection threshold on the equivalent drag coefficient is defined to reveal the abnormal flight performance caused by icing. For practical reasons, the detection is not done on the absolute value of the equivalent drag increase but on a relative value with the zero-lift drag coefficient as base. In a nominal case, the additional drag coefficient is zero and there is no relative change to the normal drag condition.

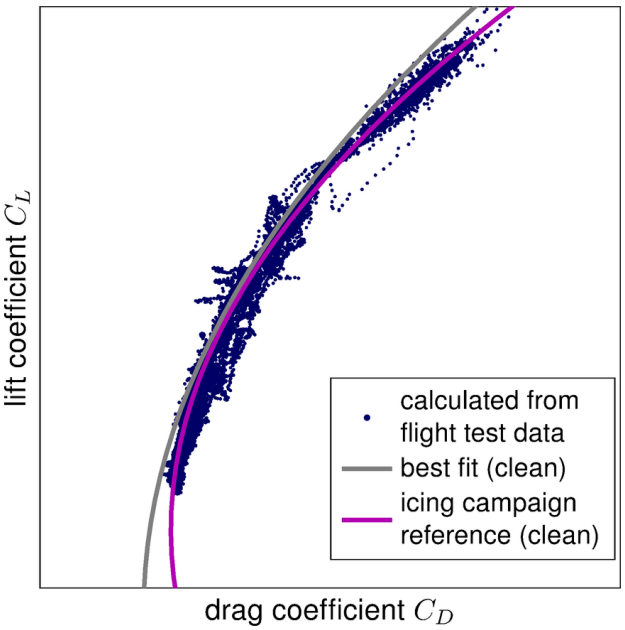

Fig. 7 Aircraft drag polar for Phenom 300 prototype used for the SENS4ICE North America icing flight test campaign: calculated lift and drag coefficient from flight test data (blue dots), pre-campaign reference drag polar (gray line, no SENS4ICE aircraft modification), and adapted campaign reference drag polar considering aircraft modifications (magenta line); clean air flight test data with aircraft in final configuration with all modification required for SENS4ICE in February 2023

During normal operation flight, there is a constant fluctuation of measured flight performance, which has to be considered by the detection algorithm through providing a suitable low-pass filtering function.In the present case, the equivalent drag coefficient data are processed by a moving average with a 8 s time window. Based on the evaluation results given in Fig. 4 for the $\mathcal{P}_{90}$ convex hull including the majority of analyzed data, the definition of the threshold is made supported by the information about the expected icing-related change of drag on the Phenom300 prototype, especially during ice build-up, which is relevant for the detection during the flight test. The variation of drag coefficient given by the $\mathcal{P}_{90}$ curve in Fig. 4 lies within a range of less than $\pm 20\% C_{D0}$, supporting the definition of a lower threshold as the implemented filters are assumed to additionally reduce the remaining variation. In addition, the implementation of a confirmation time allows further preventing false alarms caused by short-time threshold exceeding if set large enough. The confirmation time is chosen in accordance with the modeling accuracy of the whole IID system chain and quality of flight data, where high quality and accuracy of flight data measurements can lead to relatively short confirmation times and vice versa. For the detection, the confirmation time frame is chosen relatively short to ensure fast response behavior, but for reset that confirmation time must be much longer to

Table 1 Detection threshold values and confirmation time for the IID implementation: Phenom 300 prototype flight test aircraft for North America flight test campaign

Detection threshold as relative drag coefficient increase	10 %
Confirmation time frame for detection (threshold exceeded more than 50%)	20 s
Confirmation time frame for reset (threshold undershot more than 50%)	180 s

guarantee the threshold is reliably undershot and the icing-related performance degradation is not present anymore. The corresponding values are given in Table 1. The definitions of the IID configuration parameters (detection threshold, confirmation times, filter parameters) were mainly based on engineering judgment, because there were no information available prior to the flight test campaigns, which would allow a more evidence-based approach. Note that there is the expectation that the given configuration of the IID is giving fast and reliable detection information after the aircraft is affected by ice accumulation, having an announcement of the icing-related performance degradation at a time when the flight conducted at conditions where enough margin to, e.g., the maximum lift is still available and can be further conducted safely. However, with the corresponding enhanced situational awareness about the aircraft condition [7], pilots might plan their further flight differently to maintain in the safe envelope.

The IID is designed to run continuously during the whole flight and to monitor the aircraft flight performance including a potential degradation, independently from any specific flight phase or maneuver, as discussed in Ref. [7]. The SENS4ICE implementation is experimental and therefore limited to one aircraft-specific configuration defined for the flight test in icing conditions. Hence, other aircraft configurations (e.g., extended gear, deployed high-lift devices, or the usage of speed brakes) will be detected and the IID is designed to freeze and set an unreliability flag allowing the HIDS to discard the current IID output. A more detailed description is given in Ref. [8]. Note that for the consideration of additional aircraft configurations, the performance reference database must be extended accordingly.

4 Exemplary results from SENS4ICE North America flight test campaign

This paper presents initial and preliminary results from two flights of the North America icing flight test campaign. The first selected flight took place on February 23rd, 2023, departing from Chicago O'Hare Airport at 17:18UTC (11:18 local) and searching for icing conditions on the way back south to St. Louis Regional Airport in Alton, Illinois. After around 1 h of flight, the aircraft landed on St. Louis Regional Airport having successfully encountered App. C icing conditions two times during flight. Note that for the first analysis of the IID response to icing encounters during the SENS4ICE flight test campaign, there is no need to specifically focus on SLD icing cases, which are very rare and also only encountered a few times during the campaign. An overview of the flight is given in Fig. 8 including the flight track and icing encounters. Note that the information about the icing conditions found is resulting from the evaluation of atmospheric conditions measured with the following reference probes during flight: an Ice Crystal Detector (hotwire probe) for the measurement of liquid water content (LWC) and total water content, and a Cloud Combination Probe (combination of Cloud Droplet Probe (scattering probe) and Cloud Imaging Probe) for the particle-size measurements. For further details on the reference probes and measurements, the reader is referred to Ref. [37] and the references therein.

There is another example encounter presented from a flight on February 25th, 2023, departing from St. Louis Regional Airport in Alton, Illinois in a north easterly direction at 11:38 UTC (5:38 local) reaching Eugene F. Kranz Toledo Express Airport in Toledo, Ohio, at 13:42 UTC (7:42 local). During this flight SLD conditions (App. O) had been encountered near the Great Lakes.

4.1 Indirect ice detection system performance

The IID performance during this example is evaluated for the two major icing encounters in the middle of the first flight. These are visualized as time-history plots in Figs. 9 and 10. The top plot contains the altitude and indicated airspeed

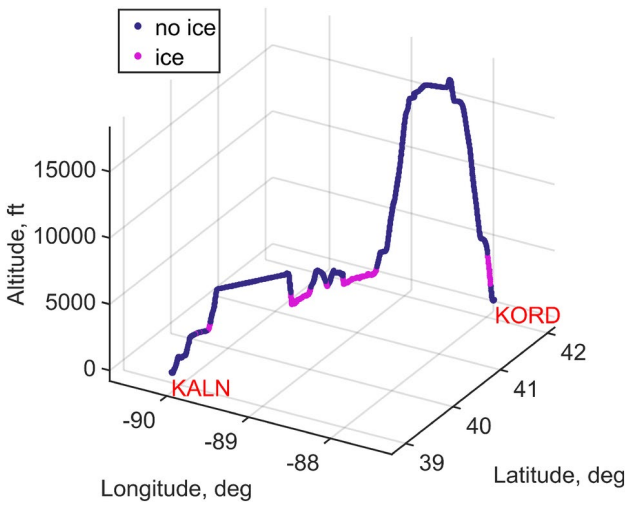

Fig. 8 Flight track from SENS4ICE North America icing campaign flight on February 23rd, 2023 (Chicago O'Hare, KORD, to St. Louis Regional Airport, KALN): geodetic position and altitude with indication of icing encountered

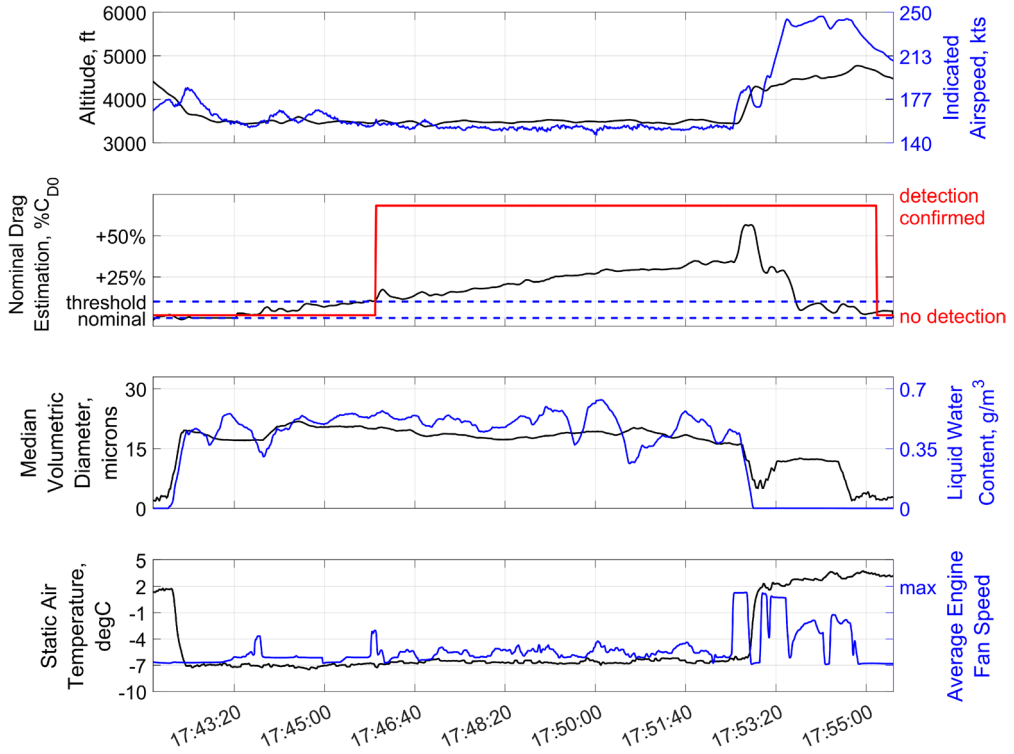

Fig. 9 Time history of IID system performance during specific icing encounter from the first example flight (17:41:49 UTC to 17:55:29 UTC): altitude and indicated airspeed (top), nominal drag estimation and IID detection output (second plot), and MVD and LWC of encountered icing conditions (third plot), and static air temperature and average engine fan speed (bottom); detection threshold at 10 % relative drag increase

for each flight segment (icing encounter). It is clearly visible that the aircraft was intentionally descending into the (expected) icing conditions and climbing again out of these after a certain encounter time. The second plot (from top) shows the nominal drag estimation (based on clean aircraft zero-lift drag) and gives a direct impression about the performance degradation. In parallel, the IID detection output is given allowing a direct comparison of drag increase and IID detection performance. Note that the shown data are a result of the online IID calculation within the HIDS system implementation directly fed with aircraft data/measurements. The third plot (from top) contains the information about the encountered icing conditions. The measured median droplet size (MVD) and liquid water content (LWC) describe the atmospheric icing conditions, in the presented case classical App. C conditions with smaller droplets. The bottom plot contains the measured static air temperature as well as the averaged engine fan speed (left and right, assuming symmetric thrust conditions). During the descend into the icing conditions, the temperature decreases significantly and increases again after leaving the conditions, indicating an atmospheric inversion layer. This allows a direct assessment about the icing encountered leading to airframe ice accretion and hence a performance degradation, together with the possibility to cross-check the detection reset (automatic change of detection flag to "no detection") with the flight through warm air and consequently de-icing. The averaged engine fan speed is directly linked to the total engine thrust and therefore gives an information about the forces applied to the aircraft in combination with the aerodynamic performance degradation.

Figure 9 shows the first icing encounter during the flight after descend to an altitude of 3,500 ft. The encounter starts at 17:42 UTC, but due to a spoiler extension in the descent phase, the IID is set to "invalid" leading to a default nominal drag estimation output, as designed, until around 17:43:20 UTC. Afterward, the airframe icing leads to a noticeable performance degradation of the aircraft at around 17:44 UTC. The detection threshold was constantly exceeded at 17:45:50 UTC causing a confirmed detection 10 s later (17:46 UTC). This means that the IID icing indication was present within 2 min after the performance degradation was starting. The performance degradation and drag was further increased during the whole encounter and reached a maximum of more than 30 % before leaving the conditions and starting the full airframe de-icing in warmer air with higher speed, leading to a detachment of all ice formation on the airframe. During climb, the reference performance

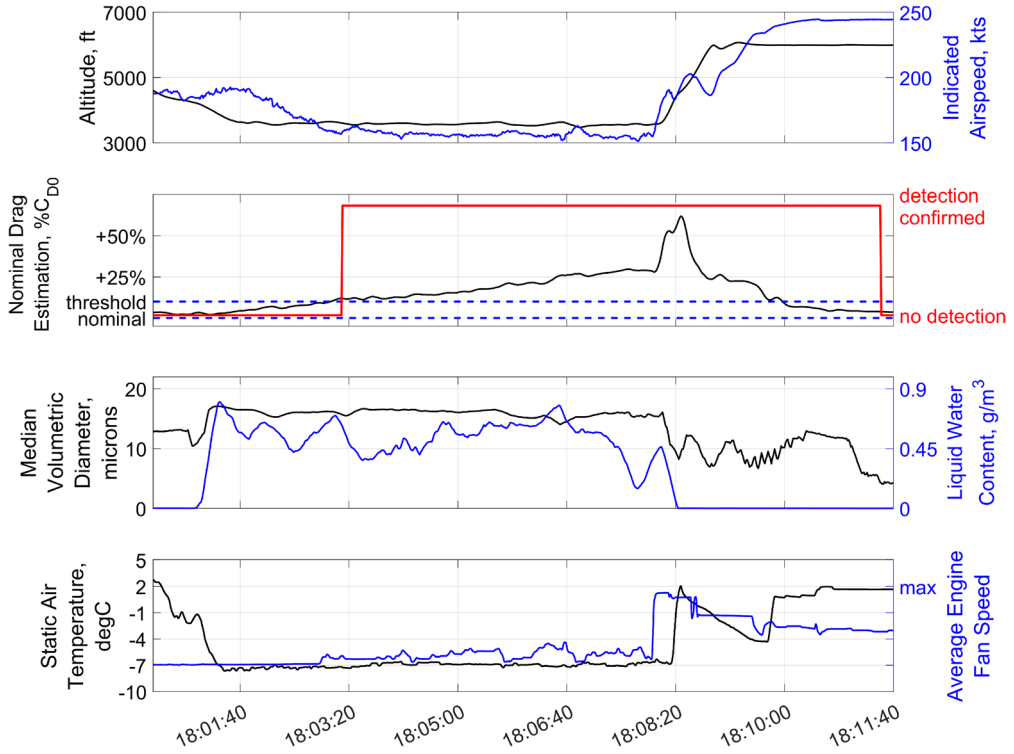

Fig. 10 Time history of IID system performance during specific icing encounter from the first example flight (18:00:19 UTC to 18:11:39 UTC): altitude and indicated airspeed (top), nominal drag estimation and IID detection output (second plot), and MVD and LWC of encountered icing conditions (third plot), and static air temperature and average engine fan speed (bottom); detection threshold at 10 % relative drag increase

of the flight test aircraft with SENS4ICE modifications was restored and the monitored degradation decreased leading to an automatic reset of the IID at around 17:55:05 UTC after the nominal drag increase undershot the threshold more the 50 % within the reset confirmation time frame; in this case around 90 s for reset.

Between 17:52:30 UTC and 17:53:10 UTC, a significant peak in the drag estimation is visible. At first sight, it seems very unrealistic that this is a consequence of the performance degradation caused by icing. Looking to the averaged engine fan speed, it becomes clear that this peak in performance degradation is directly linked to the increase of engine fan speed and therefore thrust (including the applied filtering in the IID). Knowing that the engine thrust information embedded in the IID originates from an approximation of the Pratt & Whitney PW535E engine behavior leads directly to the conclusion that the used model is not capable of correctly representing the engine thrust at the given flight condition: thrust increase at low altitude, low speed, and significant negative temperature offset ΔISA (lower temperature compared to normal conditions in the given altitude). A detailed evaluation of this behavior was part of the initial post-flight data analysis and subject to a proposal for the IID implementation modification given below in Sect. 4.3.

A similar time-history plot for the second encounter of the first example flight is given in Fig. 10. The aircraft descended into icing conditions and reached the target altitude of 3,500 ft at 18:01:40 UTC. The encounter started already during the descent leading directly to a noticeable performance degradation of around 5 % when leveling off. The drag was constantly increasing during the encounter exceeding the detection threshold at around 18:03:10 UTC. This caused a confirmed ice detection within less than 2 min after the beginning of the icing encounter. The performance degradation further increased during the flight in the icing clouds reaching again a maximum of around 30 % before the aircraft was accelerated again for climbing out the cloud layer. After reaching 6,000 ft with warmer air, the airframe was de-iced and the nominal flight performance was restored resetting the IID detection output at 18:11:30 UTC. With full engine thrust applied between 18:08:00 UTC and 18:08:40 UTC, a similar peak in the nominal drag estimation to the first encounter could be observed underpinning the above discussed finding.

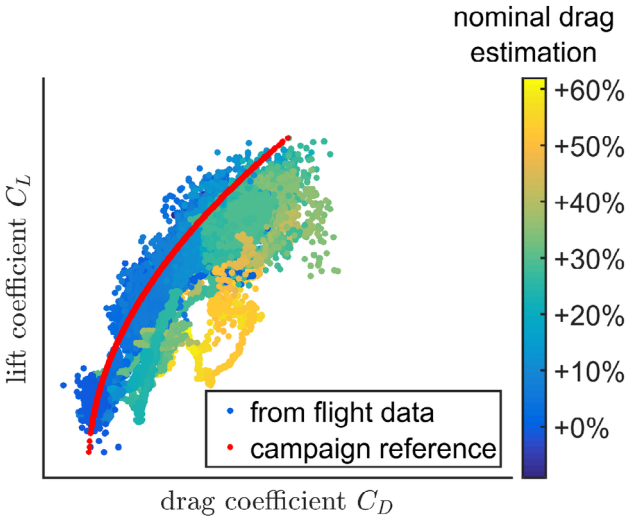

Fig. 11 Aircraft drag polar from SENS4ICE North America icing campaign flight on February 23rd, 2023 from Chicago O'Hare to Alton: calculated lift and drag coefficient from flight data measurements and drag polar reference (red line) for the Phenom 300 prototype with SENS4ICE modifications (high-lift devices and gear retracted); drag coefficient data including the indication of nominal drag estimation calculated by IID

4.2 Aerodynamic degradation due to icing

Figure 11 shows the aircraft drag polar calculated from the measured data for the whole first flight (flaps retracted, gear up, and no spoiler deflection). For each data point available in the measurement, the lift and drag coefficient is calculated based on the available inertial and inflow measurements as well as the given engine thrust model (see, e.g., Ref. [32] for detailed information on the equations). The plot further contains the aerodynamic reference used for the flight test reflecting the Phenom 300 prototype characteristics with all SENS4ICE modifications (red line). Furthermore, the drag polar data includes an indication of the corresponding IID calculated nominal drag estimation (normalized with base aircraft zero-lift drag). Blue marks indicate a nominal drag, which means that there is no increase detected. The more the aircraft is degraded, the more the drag increases and the marks are moving to the right getting lighter. Orange marks indicate the maximum calculated drag increase, which has to be taken with caution in the presented case for the already mentioned reasons. Anyway, the cyan marks show a drag increase of around 30 % (compared to the nominal value) which was approximately the maximum present during the icing encounters, as shown in Figs. 9 and 10. Without any further modifications of the IID, it can be already stated that the IID is capable of reliably and correctly indicating the current aircraft performance degradation caused by airframe icing.

Figure 12 shows the similar illustration of calculated lift and drag data, but now only for a certain selection of flight data excluding high engine fan speeds and larger negative temperature offsets (ΔISA < -5 degC). It is directly visible that the large calculated drag increase has vanished. Now a clear discrimination of clean (blue marks) and iced aircraft (cyan marks) is visible in the plot (only some orange marks indicating very large drag increase left). Hence, this underpins the above presented assumption that the used (approximated) engine thrust model over-predicts the true engine thrust in certain parts of its envelope, i.e., high engine fan speeds and large negative temperature offsets.

4.3 Post-flight IID evaluation and initial adjustment

With the first flight test data analysis available, the IID performance is further evaluated post-flight using the design model and replayed flight test data. The IID model is available for MATLAB®/Simulink including an emulation of the interface to the HIDS used during flight test. Furthermore, the IID design model allows directly accessing individual signals within the IID to further evaluate the system behavior and performance to specific influences, like the full thrust scenario which is of main concern for the initial evaluation. It also enables changes of the detection parameters, e.g., threshold and confirmation times in Table 1.

After finding that the used engine thrust model might overpredict the engine thrust sometimes, simple model adjustments were introduced to verify the assumption. It

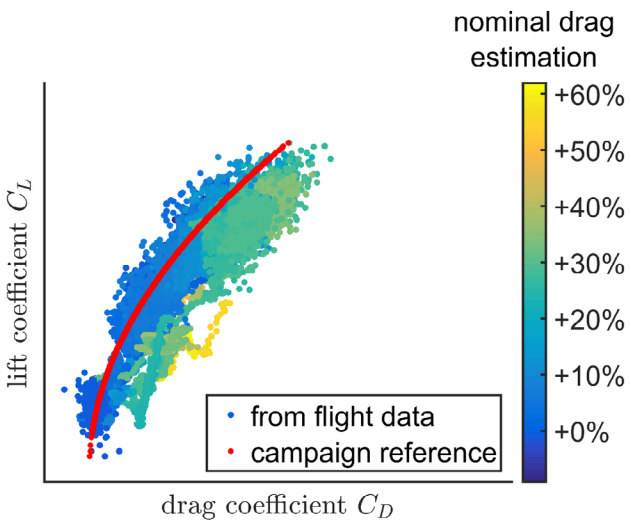

Fig. 12 Aircraft drag polar from first example flight (selected data from Fig. 11): calculated lift and drag coefficient from flight data measurements and reference for the Phenom 300 prototype with SENS4ICE modifications; data excluding high engine fan speeds N_1 and significant negative temperature offsets ΔISA; drag coefficient data including the indication of nominal drag estimation calculated by IID

is clear that the engine thrust is strongly dependent on the engine fan speed and normally shows a highly non-linear behavior for high fan speeds. Exactly, this behavior must be modified by a reduction of the maximum values without changing the engine thrust for lower fan speeds or idle. Figure 13 visualizes this required model adjustment schematically. Note that the engine thrust is further dependent on other parameters like airspeed, altitude/pressure, temperature offset, etc., which are not included in this simple figure, but expand the curve to a multi-dimensional space. The dashed line for the adjusted model indicates the slight reduction of the non-linear behavior and maximum thrust value is reduced while preserving the low fan speed behavior.

A simple linear formulation of the adjustment function allows directly achieving the new engine thrust model behavior using the original model output T_{model}

$$T_{\text{adjusted}} = T_{\text{model}} \cdot f_T + b_T \,. \tag{5}$$

During the preliminary post-flight evaluation, it was found that a few percent of reduction (values for $f_T >= 0.95$) and an offset b_T of several hundred Newton is enough to achieve much better results. Furthermore, as the data were gathered in flight from different aircraft buses with different sample rates, a suitable synchronization and therefore collinearity of data might not be given. This means that the acceleration and engine state measurement might be shifted against each other. Hence, it was further checked if the consideration of such shift in the IID process will additionally enhance the results, especially in the high thrust scenario. But it was found that such shift has no significant impact if considered to be between 0 and 100 ms in both directions.

Figure 14 contains the flight test aircraft drag polar for the whole flight including the icing encounters, now calculated with the adjusted engine thrust, similar to Fig. 11. It further contains again the flight test reference polar and an indication of the IID estimated nominal drag, this time also from a post-flight replay with the adjusted engine thrust characteristics in the performance state calculation. The maximum drag change as well as the maximum predicted performance degradation from the IID are both significantly reduced compared to the online fight test results presented in Fig. 11 as a direct consequence of the model adjustment. The maximum drag increase is limited to around 35 % which is the assumed impact of the ice formation on the airframe on the aerodynamics during the icing encounters (with still some larger values present but not affecting the IID behavior). These preliminary results give a good confidence that the source of the unreliably large drag increase is related to the full thrust scenarios.

In addition to the evaluation of the aircraft aerodynamics, the time histories of the IID performance during the encounters were analyzed. Figure 15 shows the IID output for the replayed flight test data of the first icing encounter (see Fig. 9) with the given adjustments. The calculated drag increase has changed compared to the flight test implementation by removing some peaks in the time histories correlated

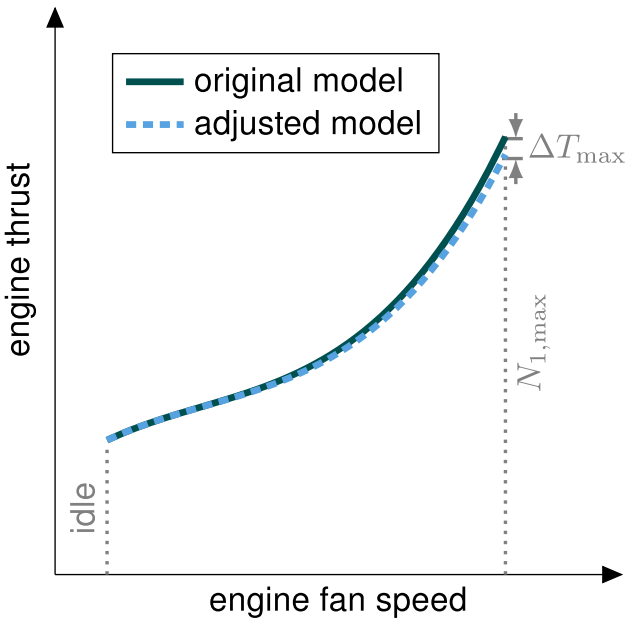

Fig. 13 Schematic illustration of engine thrust model adjustment to counteract non-linear behavior with high engine fan speeds: reduction of max. thrust with fan speeds near $N_{1,\text{max}}$ while maintaining the same thrust level for idle and medium fan speeds which correspond to the engine state for icing encounters

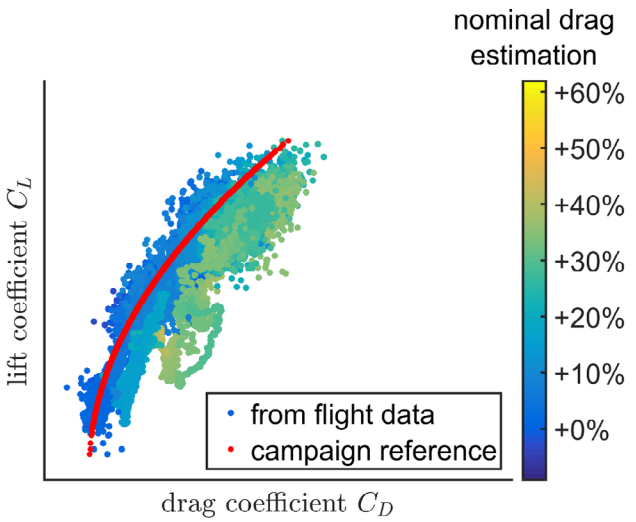

Fig. 14 Aircraft drag polar from example flight (same data as in Fig. 11) after engine thrust model adjustment: calculated lift and drag coefficient from flight data measurements and reference for the Phenom 300 prototype with SENS4ICE modifications; drag coefficient data including the indication of nominal drag estimation calculated by IID with adjusted engine thrust during data replay

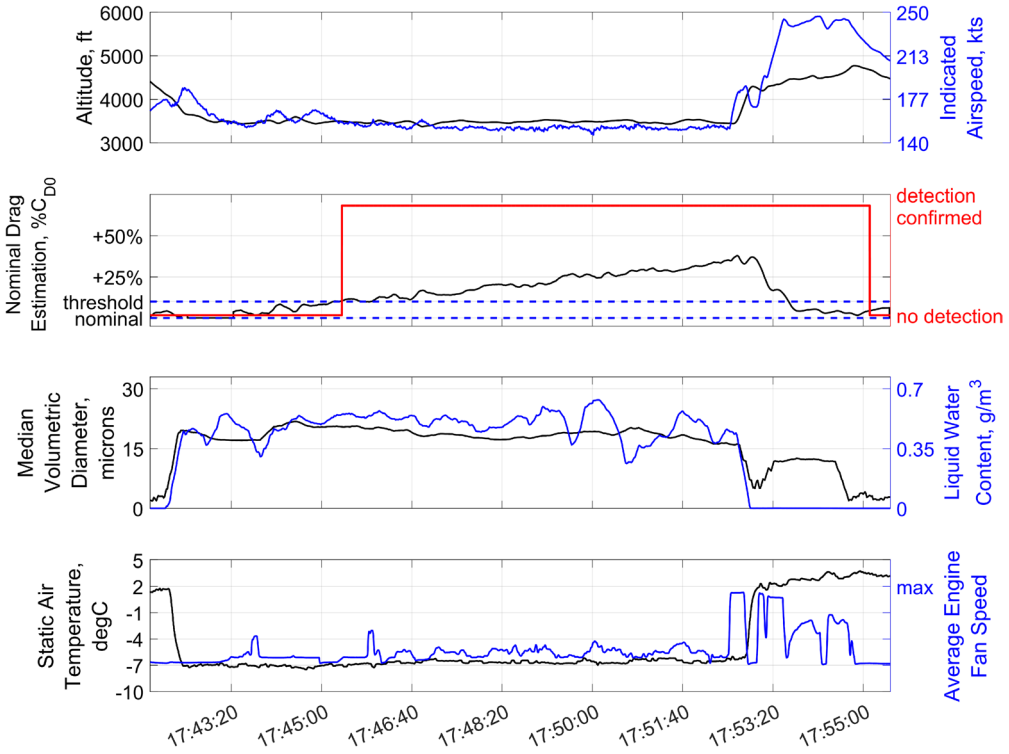

Fig. 15 Replay of IID system performance during specific icing encounter from the example flight (17:41:49 UTC to 17:55:29 UTC, see Fig. 9): altitude and indicated airspeed (top), nominal drag estimation and IID detection output (second plot), and MVD and LWC of encountered icing conditions (third plot), and static air temperature and average engine fan speed (bottom); adjusted engine thrust model behavior

with high engine fan speeds: at around 17:45:55 UTC, the engine is spooled up for a few seconds causing a small peak in the nominal drag estimation in Fig. 9 which is not existing anymore. Also, the large predicted increase starting from 17:52:30 UTC while climbing out of the icing cloud is now removed and the maximum degradation predicted by the IID remains at around 35 % which is more reasonable.

All in all, the preliminary evaluation and IID implementation adjustment revealed a very good and relatively fast detection behavior, announcing the performance degradation after the aircraft is noticeably affected by the ice accumulations. Note that the simple adjustment allows preventing some unreliable IID behavior but does not necessarily work for all conditions during all test flights. Anyway, it could be shown that the adaptation of the performance reference, of which the engine thrust model is part of, allows enhancing the IID performance and reliability if required. The flight test campaign revealed, that the engine thrust model is crucial for a good representation of the aircraft performance within the reference model and a poor engine thrust model could lead to an undesirable behavior including less accurate detections or even false alarms: if the engine thrust is underestimated, the calculated drag increase will be too low not leading directly to a positive and correct detection; if the engine thrust is predicted too high by the model (as in the presented case), the calculated drag increase is too high which leads to false alarms. Despite the specific implementation of the performance reference, e.g., multi-dimensional table for $\dot{E}_{\mathrm{tot,ref}}$ or separated aerodynamics and engine thrust, the modification to a specific aircraft is very simple and can be easily made over its lifetime in service. Hence, it is no impediment for using such a performance-based method for applications on existing aircraft or future aircraft developments.

4.4 Indirect ice detection during SLD encounter

Figure 16 contains one encounter from the second example flight on February 25th (from 13:10 UTC to 13:21 UTC) with SLDs present and a MVD above 50 microns. The aircraft descended in icing conditions and with some remaining light ice on the unprotected surfaces resulting in an already existing slight increase of estimated drag. During the encounter, the estimation exceeded the threshold at around 13:11:40 UTC until the end of the encounter with an average estimated drag increase of around 20% above nominal. In this case, the aircraft did not leave the cloud layer by a fast climb but a further descent for approaching the destination

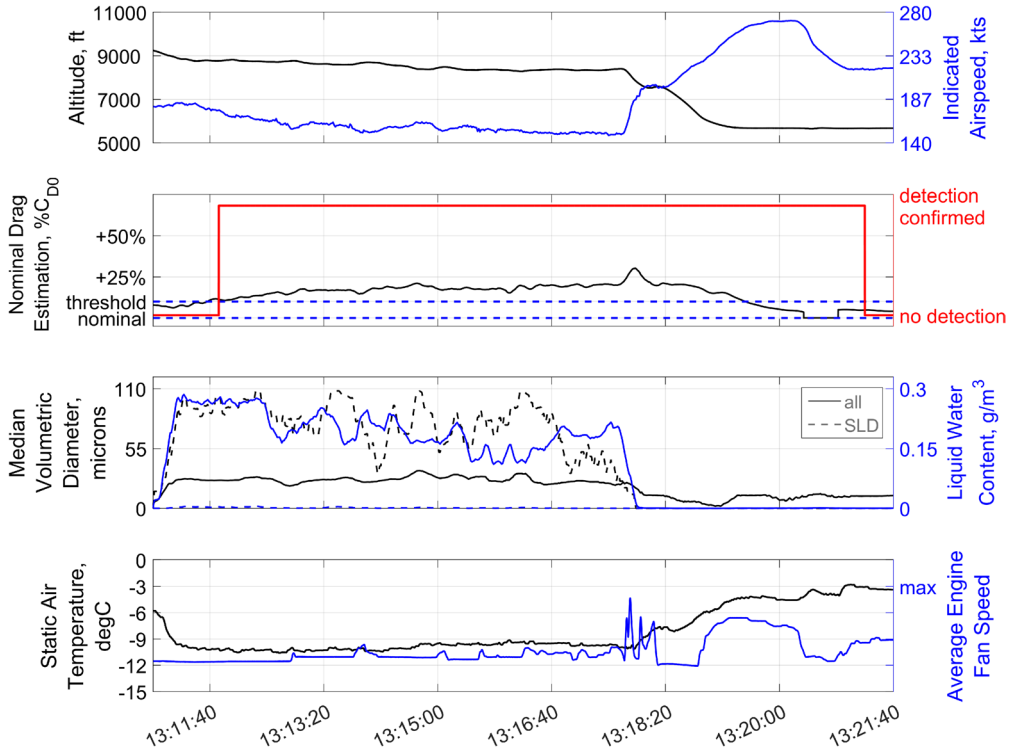

Fig. 16 Replay of IID system performance during specific icing encounter from the second example flight (13:10:49 UTC to 13:21:39 UTC): altitude and indicated airspeed (top), nominal drag estimation and IID detection output (second plot), and MVD and LWC of encountered icing conditions including indication of SLD (dashed lines) (third plot), and static air temperature and average engine fan speed (bottom); adjusted engine thrust model behavior

airport with increased speed. When leaving the cloud layer, the temperature was rising again and ice accumulation was removed. Note that the time histories presented in Fig. 16 already contain the adjusted engine model for calculating the estimated drag increase. Between 13:20 UTC and 13:21 UTC, there is a flat line in the nominal drag estimate when the spoilers were deployed to reduce the speed after leaving the clouds, which caused by default the IID to switch to "invalid" for this short time and stop the IID calculation.

5 Summary and conclusions

The SENS4ICE project is a big step toward successful and reliable detection of different icing conditions including SLD (Appendix O conditions). One key to achieve this goal is the so-called indirect ice detection methodology based on an aircraft performance degradation providing several advantages compared to direct detection (ice sensors), which are mainly complementary. These are, for example, the retrofit capabilities, a simple software solution, or the highly beneficial information about the remaining aircraft capabilities for safe aircraft operations. In addition, the indirect ice detection represents a second pillar for ice detection redundancy when hybridized and hence reduces the risk for common cause failures. It is based on the reliable measurement of the aircraft flight condition normally available through modern aircraft avionics. Furthermore, this methodology opens new possibilities for ice detection, e.g., on small unmanned aerial vehicles which could not be equipped with large or complex direct ice detection methods, but would directly benefit from a reliable and relatively fast software-based IID, giving an information about the aircraft icing situation right after the vehicle is noticeably, negatively affected.

The first results of the SENS4ICE North America flight test campaign with a specially equipped and modified Embraer Phenom 300 prototype are very promising to validate the indirect ice detection methodology and evaluate its performance during flight through natural icing conditions. It was the first time that this performance-based ice detection method was demonstrated in flight. After adaption of the performance reference, i.e., reference drag polar, based on flight data from the Phenom 300 aircraft with all SENS4ICE modifications, the IID was ready for implementation and testing during the natural icing flight test campaign. The paper presents certain preliminary results from the evaluation of one specific test flight on February 23rd, 2023, from Chicago O'Hare airport back to Alton, Illinois,

where the aircraft was stationed for the campaign. During two App. C icing encounters, the IID was able to detect the aircraft flight performance degradation caused by ice accretion on the aircraft after the icing conditions were encountered. Similarly, the presented case with SLD-icing resulted in a fast IID output after the flight performance degraded. One additional result of the evaluation is the finding that the IID implementation was very sensitive to high engine fan speeds during the flight test leading to an overprediction of the flight performance degradation. It could be shown that a simple and minor adjustment of the used engine thrust model approximation for high engine fan speeds and significant temperature offsets reduced this overpredictive behavior. In this way, it could be directly shown that an adaption of the IID to the special characteristics of one specific aircraft could be easily done based on the flight data recorded. It also revealed that the predefined structure and performance reference was successfully used to reliably indicate an abnormal aircraft performance caused by icing, even without having a perfect representation of the reference performance for all parts of the potential flight envelope. Hence, this validates the assumption that the IID can also be implemented for new aircraft designs with maybe limited information on its specific flight performance. Moreover, the presented results show that although some assumptions and approximations are made for the IID implementation, the change of aircraft flight characteristics during the icing encounter can be accurately detected within sufficient response times.

Future work on the analysis of the SENS4ICE North America flight test campaigns and the IID performance will first be dedicated to a complete evaluation of all test flights conducted in February/March 2023. In addition, a comparison of the IID performance during the European and North America campaign will further reveal the IID performance for icing encounters with different conditions and the corresponding performance degradation for a business jet and turboprop aircraft. The analysis will specifically focus on the performance degradation characteristics related to SLD ice accretion. Also, the minimal detectable ice formation through performance degradation on the different aircraft will be assessed.

6 Disclaimer

The Phenom 300 flight test data analyzed are based on an experimental prototype. This aircraft prototype has embedded additional flight test instrumentation and features that do not represent any certified Phenom 300 aircraft model. Therefore, the analysis and performance estimations assessed in this study and within the SENS4ICE project do not represent the Phenom 300's certified performance.

Acknowledgements The author wants to specially thank the SENS4ICE North America campaign flight test team for its structured and professional work to conduct the flight tests, especially Daniel Martins da Silva for coordinating with the SENS4ICE project group. Furthermore, the author wants to specially honor the work of Bruno Thillays and Annagrazia Orazzo from SAFRAN Aerosystems on developing the HIDS implementation for the SENS4ICE flight tests.

Author contributions C.D. wrote the paper as sole author.

Funding Open Access funding enabled and organized by Projekt DEAL. The "SENSors and certifiable hybrid architectures for safer aviation in ICing Environment" (SENS4ICE) project has received funding from the European Union's Horizon 2020 research and innovation program under Grant Agreement No.$$N^\circ$$ 824253.

Data availability No datasets were generated or analyzed during the current study.

Declarations

Conflict of interest The author has no conflict of interest to declare that are relevant to the content of this article.

References

1. Green, S.D.: A study of U.S. inflight icing accidents and incidents, 1978 to 2002. Number AIAA 2006–82, Reno, Nevada, USA, January 9th - 12th. In: 44th AIAA Aerospace Sciences Meeting and Exhibit, American Institute of Aeronautics and Astronautics. Inc. (AIAA). (2006). https://doi.org/10.2514/6.2006-82
2. Green, S.D.: The icemaster database and an analysis of aircraft aerodynamic icing accidents and incidents. Technical Report DOT/FAA/TC-14/44, R1, Federal Aviation Administration, Atlantic City, NJ, USA, Oct. (2015)
3. Anon.: *Final Report (BFU 5X011-0/98)*. German Federal Bureau of Aircraft Accident Investigation, Braunschweig, Germany, April (2001)
4. Anon.: *Aircraft Accident Report (NTSB/AAR-96/01, DCA95MA001), Safety Board Report*. National Transportation Safety Board (NTSB), Washington, DC, USA, July 9th (1996)
5. Anon.: Certification specifications and acceptable means of compliance for large aeroplanes (CS-25). Amendment 28 (current version, European Union Aviation Safety Agency (EASA), Cologne, Germany, December, 15th (2023)
6. Anon.: Certification specifications and acceptable means of compliance for large aeroplanes (CS-25). Amendment 16, European Union Aviation Safety Agency (EASA), Cologne, Germany, March, 12th (2015)

7. Christoph, Deiler, Nicolas, Fezans: Performance-based ice detection methodology. J. Aircr. **57**(2), 209–223 (2020). https://doi.org/10.2514/1.C034828
8. Deiler, C., Sachs, F.: Design and testing of an indirect ice detection methodology. Vienna, Austria, June 20th - 22nd 2023. In: SAE International Conference on Icing of Aircraft, Engines, and Structures, SAE International, Paper 2023-01-1493 (2023) https://doi.org/10.4271/2023-01-1493
9. Schwarz, C.W.: The SENS4ICE EU project – SENSors and certifiable hybrid architectures for safer aviation in ICing Environment – project overview and initial results. Stockholm, Sweden, September 4th–9th . 33th Congress of the International Council of the Aeronautical Sciences (ICAS). (2022) https://icas.org/ICAS_ARCHIVE/ICAS2022/data/papers/ICAS2022_0794_paper.pdf
10. Schwarz, Carsten: SENS4ICE EU project preliminary results. SAE Int. J. Adv. Curr. Pract. Mobil. **6**(3), 1140–1149 (2023). https://doi.org/10.4271/2023-01-1496
11. Zollo, A.L., Bucchignani, E.: An aviation support tool for satellite remote detection of in-flight icing. Bratislava, Slovakia, 4th – 8th September 2023. EMS Annual Meeting. (2023) https://doi.org/10.5194/ems2023-297
12. Zollo, A.L., Bucchignani, E.: A tool for remote detection and nowcasting of in-flight icing using satellite data. Vienna, Austria, June 20th–22nd 2023. In: SAE International Conference on Icing of Aircraft, Engines, and Structures, SAE International, Paper 2023-01-1489 (2023) https://doi.org/10.4271/2023-01-1489
13. Gonzalez, M., Frövel, M.: Fiber bragg grating sensors ice detection: methodologies and performance. Sens. Actuators A Phys. **346**, 113778 (2022). https://doi.org/10.1016/j.sna.2022.113778
14. Pohl, M., Feder, J., Riemenschneider, J.: Lamb-wave and impedance based ice accretion sensing on airfoil structures. In: Su, Z., Glisic, B., Limongelli, M.P. (eds.), Sensors and Smart Structures Technologies for Civil, Mechanical, and Aerospace Systems 2023, vol. 12486, p. 124860Y. International Society for Optics and Photonics, SPIE, (2023). https://doi.org/10.1117/12.2658311
15. Deiler, C., Schwarz, C., Ridouane, E.H., Orazzo, A., Jurkat-Witchas, T., et. al.: Final report on evaluation of technologies developed in SENS4ICE and technical project results. Final report D4.4, German Aerospace Center (DLR), Braunschweig, Germany, February 6th (2024). https://www.sens4ice-project.eu/sites/sens4ice/files/media/2024-02/SENS4ICE_D4.4_Final_Report_DLR_20240131_v2.pdf
16. Jurkat-Witschas, T., Lucke, J., Schwarz, C.W., Deiler, C., Sachs, F., Kirschler, S., Menekay, D., Voigt, C., Bernstein, B., Jaron, O., Kalinka, F., Zollo, A., Lilie, L., Mayer, J., Page, C., Vié, B., Bourdon, A., Pereira Lima, R., Vieira, L.: Overview of cloud microphysical measurements during the SENS4ICE airborne test campaigns: Contrasting icing frequencies from climatological data to first results from airborne observations. Vienna, Austria, June 20th - 22nd 2023. In: SAE International Conference on Icing of Aircraft, Engines, and Structures, SAE International, Paper 2023-01-1491 (2023)
17. Deiler, C.: Performance-based ice detection first results from SENS4ICE european flight test campaign. Orlando, Florida, USA,: AIAA Scitech Forum, American Institute of Aeronautics and Astronautics. Inc. (AIAA). (2024). https://doi.org/10.2514/6.2024-2817
18. Wagner, B., Hammond, D.W., van Hengst, J., Gent, R.W., Kind, R.J.: Ice accretion simulation - Chapter 1. AGARD Advisory Report 344, Advisory Group for Aerospace Research & Development (AGARD) - Fluid Dynamics Panel Working Group 20, North Atlantic Treaty Organization (NATO), Neuilly-Sur-Seine, France, December (1997)
19. Bragg, M.B., Perkins, W.R., Sarter, N.B., Başar, T., Voulgaris, P.G., Gurbacki, H.M., Melody, J.W., McCray, S.A.: An interdisciplinary approach to inflight aircraft icing safety. Number AIAA 98–0095, Reno, Nevada, USA, January 12th-15th. In: 36th AIAA Aerospace Sciences Meeting and Exhibit, American Institute of Aeronautics and Astronautics. Inc. (AIAA). (1998). https://doi.org/10.2514/6.1998-95
20. Myers, T.T., Klyde, D.H., Magdaleno, R.E.: The dynamic icing detection system (DIDS). Reno, Nevada, USA, January 10th - 13th. In: 38th AIAA Aerospace Sciences Meeting and Exhibit, American Institute of Aeronautics and Astronautics. Inc. (AIAA) (1999). https://doi.org/10.2514/6.2000-364
21. Melody, James W., Başar, Tamer, Perkins, William R., Voulgaris, Petros G.: Parameter identification for inflight detection and characterization of aircraft icing. Control. Eng. Pract. **8**(9), 985–1001 (2000). https://doi.org/10.1016/S0967-0661(00)00046-0
22. Bragg, M.B., Başar, T., Perkins, W.R., Selig, M.S., Voulgaris, P.G., Melody, J.W., Sater, N.B.: Smart icing systems for aircraft icing safety. Reno, Nevada, USA, January 14th - 17th. In: 40th AIAA Aerospace Sciences Meeting and Exhibit, American Institute of Aeronautics and Astronautics. Inc. (AIAA). (2002). https://doi.org/10.2514/6.2002-813
23. Aykan, R., Hajiyev, C., Caliskan, F.: Aircraft icing detection, identification and reconfigurable control based on kalman filtering and neural networks. San Francisco, California, USA, August 15th - 18th. In: AIAA Atmospheric Flight Mechanics Conference and Exhibit, American Institute of Aeronautics and Astronautics. Inc. (AIAA). (2005). https://doi.org/10.2514/6.2005-6220
24. Gingras, D.R., Barnhart, B.P., Ranuado, R.J., Ratvasky, T.P., Morelli, E.A.: Envelope protection for in-flight ice contamination. Orlando, Florida, USA, January 5th - 8th. In: 47th Aerospace Sciences Meeting, American Institute of Aeronautics and Astronautics. Inc. (AIAA). (2009). https://doi.org/10.2514/6.2009-1458
25. Deiler, C., Ohme, P., Raab, C., Mendonca, C., Silva, D.: Facing the challenges of supercooled large droplet icing: Results of a flight test based joint dlr-embraer research project. SAE Int. J. Adv. Curr. Pract. Mobil. **2**(1), 192–204 (2020). https://doi.org/10.4271/2019-01-1988
26. Deiler, Christoph: Comparison of flight characteristics of two different airplanes and ice configurations. J. Aircr. **57**(5), 995–1000 (2020). https://doi.org/10.2514/1.C035801
27. Morelli, Eugene, Grauer, Jared: Advances in aircraft system identification at nasa langley research center. J. Aircr. **60**(5), 1354–1370 (2023). https://doi.org/10.2514/1.C037274
28. Deiler, C.: Evaluation of aircraft performance variation during daily flight operations. Friedrichshafen, Germany, Sept. 2018. Deutscher Luft- und Raumfahrtkongress, Deutsche Gesellschaft für Luft- und Raumfahrt (DGLR) (2018) https://doi.org/10.25967/480025
29. Christoph, Deiler: Aerodynamic modeling, system identification, and analysis of iced aircraft configurations. J. Aircr. **55**(1), 145–161 (2018). https://doi.org/10.2514/1.C034390
30. Deiler, Christoph: Flight characteristics with different supercooled large droplet ice configurations. Aeronaut. J. **126**, 848–865 (2022). https://doi.org/10.1017/aer.2021.98
31. Deiler, C., Fezans, N.: Performance-based ice detection methodology. Denver, Colorado, USA, June 5th - 9th. In: Atmospheric Flight Mechanics Conference, AIAA Aviation Forum and Exhibition, American Institute of Aeronautics and Astronautics. Inc. (AIAA) (2017) https://doi.org/10.2514/6.2017-3394
32. Deiler, C.: A smart data approach to determine an aircraft performance model from an operational flight data base. National Harbor, Maryland, USA,: AIAA Scitech Forum, American Institute of Aeronautics and Astronautics. Inc. (AIAA) (2023) https://doi.org/10.2514/6.2023-0797

33. Deiler, Christoph: Engine thrust model determination and analysis using a large operational flight database. CEAS Aeronaut. J. **14**(1), 29–45 (2023). https://doi.org/10.1007/s13272-023-00659-w
34. Deiler, Christoph: Aerodynamic model adjustment for an accurate flight performance representation using a large operational flight data base. CEAS Aeronaut. J. **14**(2), 527–538 (2023). https://doi.org/10.1007/s13272-022-00625-y
35. Deiler, C., Fezans, N.: Method and assistance system for detecting a degradation of flight performance, 2017. Patent Numbers: US11401044B2, EP3479181B1, WO2018002148A1, FR3053460B1, CA3029467A1, ES2919573T3
36. Orazzo, A., Thillays, B., Deiler, C.: Final report on hybrid ice detection development. Final report D4.2, SAFRAN Aerosystems, Plaisir, France, February 6th 2024. https://www.sens4ice-project.eu/sites/sens4ice/files/media/2024-02/SENS4ICE_D4.2_Final_report_on_HIDS_development_Safran_20240201.pdf
37. Lucke, J., Jurkat-Witschas, T., Menekay, D., Bernstein, B.C., Garcia, G.S., Jaron, O., Bourdon, A., Voigt, C.: Occurrence and properties of supercooled large droplet icing conditions in low and mid-level clouds as observed during the sens4ice campaigns over north America and Europe. AIAA Aviation Forum and Ascend, Las Vegas, Nevada, USA, July 29th - August 2nd. In: American Institute of Aeronautics and Astronautics. Inc. (AIAA). (2024). https://doi.org/10.2514/6.2024-3526